JOURNAL OF PHYSICAL ORGANIC CHEMISTRY, VOL. 6, 113–121 (1993)

CATALYTIC ACTIVITY OF POLYPODANDS AND GLYMES UNDER SOLID–LIQUID PHASE-TRANSFER CATALYSIS CONDITIONS. A MOLECULAR MECHANICS STUDY

A. A. VARNEK,* A. MAIA AND D. LANDINI
Centro CNR and Dipartimento di Chimica Organica e Industriale, Università di Milano, Via Golgi 19, I-20133 Milan, Italy
A. GAMBA AND G. MOROSI
Centro CNR and Dipartimento di Chimica Fisica ed Elettrochimica, Universitá di Milano, Via Golgi 19, I-20133 Milan, Italy
AND
G. PODDA
Dipartimento Farmaco Chimico Tecnologico, Università di Cagliari, Via Ospedale 72, I-09124 Cagliari, Italy

A molecular mechanics study of cyclophosphazenic polypodands and of glymes, of their complexes with ion pairs (IPs) M^+I^- ($M^+ = Li^+, Na^+, K^+, Rb^+$) and IP aggregates $(M^+I^-)_n$ was carried out to investigate the catalytic activity of these ligands in solid–liquid phase-transfer reactions. This activity is explained by their ability to bind IP aggregates effectively and to activate the anion by increasing the interionic distance in the single IP.

INTRODUCTION

Polypodands are acyclic molecules that contain a number of polyether chains, linked to the same molecular fragment. They are known as effective complexation agents for alkali and alkaline earth metal salts, even in low-polarity media,[1] and hence they can be used as catalysts in phase-transfer processes.[1,2] Recently, we showed[3] that cyclophosphazenic polypodands **1a–c** behave as efficient catalysts in a number of anion-promoted reactions under solid–liquid phase-transfer catalysis (SL-PTC) conditions and that their catalytic activity is much higher than that exhibited by the simple glyme **2** and the tris(polyoxaalkyl)amine 'TRIDENT' (**3**).[3b]

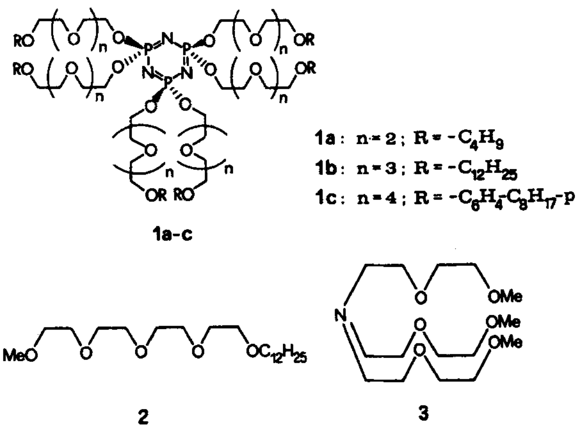

Scheme 1

In particular, the study of the extent of complexation of **1–3** and of their catalytic efficiency in a typical nucleophilic substitution reaction:

$$n\text{-}C_8H_{17}OSO_2CH_3 + (M^+Y^-)_{solid} \xrightarrow[C_6H_5Cl,\ 60\,^\circ C]{Lig(cat)} n\text{-}C_8H_{17}Y + (CH_3SO_3^-M^+)_{solid} \quad (1)$$

where Lig = **1a–c**, **2**, **3**, $M^+ = Li^+, Na^+, K^+, Rb^+$ and $Y^- = SCN^-, I^-, Br^-$, under SL-PTC conditions evidenced the following specific features. (i) The number of moles of complexed salt n per mole of ligand in the Ligand–$(M^+Y^-)_n$ complex decreases according to the sequence **1c** ⩾ **1b** > **1a** > **3** > **2**, and depends strongly on the nature both of the cation and the anion. Thus in the complexes of **1c** with alkali metal iodides n is equal

---

* Permanent address: Mendeleev Institute of Chemical Technology, Miusskaya Sq. 9, Moscow 125820, Russia.

0894–3230/93/020113–09$09.50

Received 23 March 1992
Revised 7 September 1992

to 17, 4, 1 and 0·6 for Li^+, Na^+, K^+ and Rb^+ respectively. The cation being the same, the *n* value decreases in the order $SCN^- > I^- \gg Br^- > Cl^-$. (ii) The catalytic activity in reaction (1) is largely determined by the complexing ability of these ligands, i.e. **1c** ⩾ **1b** > **1a** > **3** > **2**.

The mechanism of nucleophilic substitution reactions catalysed by neutral phase-transfer agents under SL-PTC conditions, as in reaction (1), has not so far been as well defined as that of similar reactions in liquid–liquid two-phase systems.[2] In particular, the data concerning ligands **1**–**3** are rationalized with some difficulty.

Reasonable hypotheses can be formulated on the basis of the data obtained by Yufit and Esikova[4] in Finkelstein solid–liquid reactions promoted by quaternary ammonium halides. They showed[4] that vigorous stirring of the heterogeneous mixture leads to the formation of subcolloidal particles of the solid phase of small size (for example, the side at the equivalent cubic block for KCl is less than 24 nm), so allowing the reaction to proceed.

In addition to the increase in the solid-phase surface, the mechanical activation of the SL system generates a number of defects in the crystals. This is assumed to facilitate the transfer of salt fragments into solution, according to the equilibrium

$$(M^+Y^-)_{solid} \rightleftharpoons [(M^+Y^-)_n]_{solv} \qquad (2)$$

Owing to the low solvation ability of the solvent used, aggregates $(M^+Y^-)_n$ should be localized near the solid-phase surface. In agreement with this assumption, IR spectroscopic studies[5] evidenced the presence of ion pairs (IPs) and IP aggregates with $n = 2$–8 for thiocyanates, perchlorates and nitrates of Li, Na and K in solvents with low dielectric constant such as ethyl acetoacetate, tributyl phosphate and tetrahydrofuran ($\varepsilon = 6$–8);[6] the extent of IP aggregation decreases in the order $Li^+ > Na^+ > K^+$.[5]

Analogously, we can assume that also in chlorobenzene ($\varepsilon = 5{\cdot}68$) the mechanical activation of reaction (1) promoted by the ligands **1**–**3** leads to the formation of subcolloidal particles $(M^+Y^+)_{solid}$ and aggregates $(M^+Y^-)_n$. In this case polypodands or glymes can interact with the IP aggregates, activating the anion.

In order to investigate these processes, the method of molecular mechanics was used to study the structural and energy properties of the complexes of some glymes and podands with ion pairs M^+I^- and their aggregates $(M^+I^-)_n$. The following compounds were chosen as models in the present investigation: a molecule similar to **1c**, but with R = Ph(POD); three glymes with 4 to 6 oxygen atoms, i.e. $EtO(C_2H_4O)_3Et$ (GLYME4), $MeO(C_2H_4O)_4Et$ (GLYME5) and $MeO(C_2H_4O)_5Ph$ (GLYME6); and the ion pair M^+I^- and its aggregate $(M^+I^-)_n$ simulating a salt fragment.

EXPERIMENTAL

Conformational calculations on polypodands, glymes and their complexes with IPs and IP aggregates were performed by the molecular mechanics method using the MM2I program.[7] This package computes the intramolecular interactions by the Allinger force field.[8] Some previously unknown parameters, required for the description of the POD molecule, were determined in such a way as to reproduce the experimental geometries of cyclotriphosphazenic derivatives obtained by x-ray[9] and electron diffraction methods[10] (see Table 1).

The MM2I program evaluates ion–molecule and intermolecular interactions by a modified[7] force field[11,12] which represents the intermolecular interaction energy as a sum of electrostatic, polarization and van der Waals terms.

The electrostatic term is calculated in the point-charge approximation, the atomic charges Q_i being determined in such a way as to reproduce the molecular electrostatic potential distribution (PD charges[13]) on the Connolly surfaces,[14] computed by the MNDO method using the MOPAC-5 package.[15] The charges were multiplied by the factor 1·42, which scales the MNDO PD charges to the *ab initio* (6–31G*) values.[16]

Our molecules are not suitable for a direct calculation of PD charges, owing to the close dependence of Q_i values on the molecular geometry;[17] we therefore used by-fragment calculations[18] with further averaging of Q_i. PD charges for *N* (−1·2) and *P* (1·8) were obtained in calculations on the hexamethoxycyclotriphosphazene. The averaged values for the atoms of the polyether chains $C_2H_5O(C_2H_4O)_nC_2H_5$, $n = 1$–3, are −0·6 (O), 0·3 (C) and 0·0 (H).[19] For the phenyl group, which is connected to the polyether chain, the PD charges are 0·5, −0·4, −0·1, −0·2, −0·4, −0·1 for the carbons, starting from the carbon bonded to the oxygen, and 0·2 for the hydrogens.

The polarization term is computed[11] using data on bond polarizabilities.[20]

The van der Waals interaction energy is calculated by the equation

$$E_{vdw} = \sum_i \sum_j k_{ij} \times \left[-\frac{A}{Z_{ij}^6} + \left(1 - \frac{Q_i}{N_i}\right)\left(1 - \frac{Q_j}{N_j}\right) B_0 \exp(-\alpha Z_{ij}) \right] \qquad (3)$$

Table 1. Geometrical data for cyclotriphosphazenic derivatives

	Bond length (Å)		Bond angle (°)	
	P=N	P—O	P—N—P	P—O—C
Calc.	1·58	1·58–1·59	119–122	117–119
Exp.[9,10]	1·56–1·60	1·56–1·59	120–123	120–131

Table 2. Geometrical and energy data for alkali metal iodides

	Bond length (Å) in single IP		Bond length (Å) in crystal		Lattice energy per IP (k cal mol^{-1})^{b}	
Cation	Calc	Exp.[22]	Calc.^{a}	Exp.[23]	Calc.^{a}	Exp.[23]
Li^+	2·448	2·392	3·08	3·006	103·5	101·3
Na^+	2·718	2·711	3·35	3·239	96·3	94·4
K^+	3·044	3·048	3·56	3·533	89·2	87·6
Rb^+	3·175	3·177	3·63	3·670	87·2	85·3

[a] Averaged value.
[b] Using the Madelung constant $k = 1·7476$.

where Z_{ij} is the scaled interatomic distance, N_i the number of valence electrons of the atom i and A, B_0 and α are fixed parameters.[11] For the interactions of C, H, O, N and P with M^+ we used standard k_{ij} values,[12,19,21] while for the interaction with I^- the constants were set equal to 1·0. The k_{ij} values for the M^+–I^- interactions were fitted both to the bond lengths in the gas phase and to the interionic distances and the lattice energy in the crystal, the two systems being modelled by a single IP and a three-dimensional cluster $(M^+I^-)_{24}$, respectively. The results in Table 2 show that the parameters reproduce reliably the structural and energetic properties of the models.

This force field combination allows complicated systems to be modelled, including several interacting partners, namely ligands, cations, anions and a few solvent molecules, and takes into account non-additivity effects. Its reliability was confirmed by the results on the geometry and the energy of crown ethers and organophosphorus podands and of their complexes with alkali metal cations and ion pairs.[19,21]

RESULTS AND DISCUSSION

Glymes

The starting conformations of glymes were generated by setting the COCC torsion angles to their optimum value of 180°[24] and the OCCO angles to 180 or ±60°. All the possible conformations were analysed, considering all the C—O bonds in *trans* (TTT...) and *gauche* (GG^-G...), and combinations of *trans* and *gauche* angles (TTG ..., TGT ..., G^-TG ...).

The optimized geometries of the glyme complexes with IPs and with their aggregates show the following general features. (i) The least effective interaction with IPs occurs for all *trans* (TTT ...) conformations, when each cation coordinates one oxygen atom only. (ii) The interaction with one IP of a chain with *gauche* torsion angles produces a cooperative effect. If there is an alternation of *trans* and *gauche* angles in the chain (GTG^- ..., GTG ..., etc.), the oxygens, in *gauche* positions to each other, can interact simultaneously with the same cation, that is, they form a chelating bonding site (BS). Chains with a consecutive arrangement of *gauche* (+) and *gauche* (−) angles (GG^-GG^- ...) form BSs including up to six oxygens (conformation GG^-GG^-G, GLYME6). (iii) When IPs and their aggregates interact with chains containing chelating BSs, the OCCO torsion angles fall to 30–40°, that is, the planarity of a chain fragment increases. A chelating BS coordinates only one cation, so, if the number of IPs is larger than the number of BSs, the excess IPs are bound to those already coordinated. Aggregates $(M^+I^-)_2$, $(M^+I^-)_4$, $(M^+I^-)_6$ interact with chelating BSs through one of the cations.

More complex structures are shown by GLYME5 (GG^-GG^-) and GLYME6 (GG^-GG^-G) complexes.

The molecule GLYME5 (GG^-GG^-) binds effectively two IPs. Each cation of the lithium iodide complex [Figure 1(a)] coordinates four oxygens; three of them, lying in a plane perpendicular to the line connecting the Li^+ atoms, are near to the cation, whereas the last one is far apart. The distance between the cations is small (2·68 Å), but the repulsion between IPs is compensated for by their interaction with the ligand. Such a coordination of IPs is energetically more favourable than the complex ($TGTG^-$), where each cation coordinates the oxygen atoms of its own chelating BS [Figure 1(b)], the total energies being −376·2 and −316·8 kcal mol^{-1}, respectively, (1 kcal = 4·184 kJ).

The molecule GLYME6 interacts with IPs more effectively in its GG^-GG^-G conformation. In the complex with Li^+I^- and Na^+I^- the BS is formed by all six oxygens of the chain (pseudo-cavity conformation). The cation coordination polyhedron is a trigonal prism with cation–oxygen distances equal to 1·96–2·06 Å (Li^+I^-) and 2·22–2·34 Å (Na^+I^-). In the complexes with K^+I^- and Rb^+I^-, the cation coordinates five oxygens with $M^+\cdots O$ distances equal to 2·73–2·78 Å

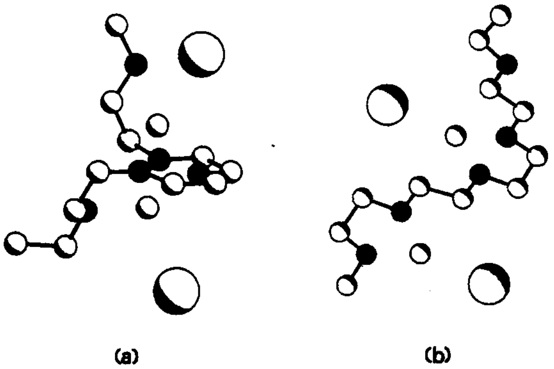

Figure 1. Complexes of Li^+I^- with the (a) (GG^-GG^-) and (b) ($TGTG^-$) conformers of GLYME5

(K^+I^-) and 3·00–3·08 Å (Rb^+I^-), while the distances of the sixth oxygen are larger [4·71 Å (K^+I^-) and 4·87 Å (Rb^+I^-)]. Specific features of these GLYME6–M^+I^- complexes are not only the strong cation–ligand interaction, but also the expulsion of the anion from the pseudo-cavity following the increase in the cation–anion distance (Table 3). This effect is present in the complex with Li^+I^- [Figure 2(a)] and Na^+I^-, where the cation–anion distances are increased by 3·28 and 2·61 Å, respectively, whereas it is negligible in K^+I^- (0·24 Å) [Figure 2(b)] and Rb^+I^- (0·18 Å).

It it noteworthy that other conformations do not show large variations of IP bond lengths.

Polypodands

The number of possible conformers of the polypodands with long polyether chains is so large that we could not afford a systematic scanning of the whole conformational space. Therefore, the simulation was carried out by selecting sequences of BSs for the polyether chains bound to the cyclotriphosphazenic (CTP) fragment and by optimizing the geometry.

Table 3. Cation–ligand, $E_{L\cdots M^+}$, anion–ligand, $E_{L\cdots I^-}$, and cation–anion, $E_{M^+\cdots I^-}$, interaction energies (kcal mol^{-1}) and cation–anion distances, $R_{M^+\cdots I^-}$ (Å), in the complexes of GLYME6 (pseudo-cavity conformation) with alkali metal iodide ion pairs

Cation	$E_{L\cdots M^+}$	$E_{L\cdots I^-}$	$E_{M^+\cdots I^-}$	$R_{M^+\cdots I^-}$
Li^+	−207·9	−7·9	−58·0	5·73 (2·45)[a]
Na^+	−153·2	−9·7	−62·3	5·33 (2·72)[a]
K^+	−87·8	10·0	−95·3	3·28 (3·04)[a]
Rb^+	−73·1	10·3	−92·4	3·36 (3·18)[a]

[a] Values in parentheses: in the isolated IP.

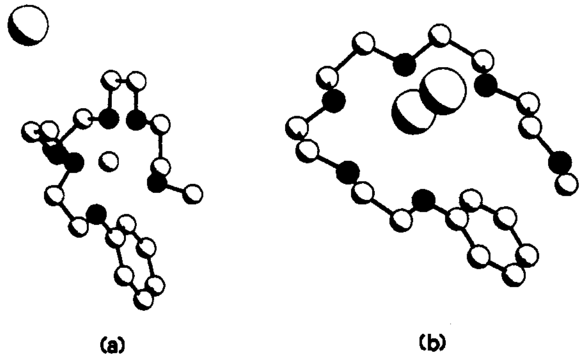
(a) (b)

Figure 2. Complexes of (a) Li^+I^- and (b) K^+I^- with GLYME6

The polypodand conformation is described assigning to each conformer a 'conformation type,' according to the classification $n_1(X_{m_1})n_2(Y_{m_2}), \ldots, n_i(Z_{m_i}), \ldots$, where n_i is the number of polyether chains of X type; X is the BS type, defined by the number of oxygen atoms (N_O) forming it:

N_O	1	2	3	4	5	6
X	M (Mono)	B (Bi)	T (Tri)	Te (Tetra)	P (Penta)	H (Hexa)

and m_i is the number of BSs in the chain.

The sequence of OCCO torsion angles in the polyether chains, the conformation type and the steric energy (E_{st}) are reported in Table 4. The most stable conformer is $6P_1$ [Figure 3(a)], in which each chain forms a BS including five oxygen atoms. Attempts to simulate the $6H_1$ conformer, with six donor atoms in a BS, failed owing to the high steric tension of the molecule, and any substitution of the pentadentate BS with a set of smaller BSs increases the steric energy. The E_{st} value is determined not only by the position of the BS in the chain, but also by the sign of corresponding OCCO torsion angle: a comparison of the data of five conformers of $6B_2$ type (see Table 4) shows that a change from G to G^- induces a very small variation of E_{st} in the complexes with chelating BSs formed by the 3–4 and 5–6 oxygens, but if the BSs are moved to the 2–3 and 4–5 oxygens, the steric energy not only increases, but also becomes significantly dependent on the substitution of G by G^-. The more deeply the IP is bound inside the cavity formed by the chains, the stronger is the deformation of the molecule and the less flexible it is. On the whole, the results confirm the well known fact[25] that the *gauche* conformation of OCCO fragment is more stable than the *trans* conformation.

The polypodands are 'octopus-like' molecules, different orientations and bendings of the 'octopus tentacles' corresponding to different conformers. All the possible conformations can be grouped according to their ability to bind IP aggregates. Some conformers,

Table 4. POD conformations and steric energies (kcal mol^{-1})

Chain conformation	Conformational type	BS positions	E_{st}
GTGTG	$6B_3$	1–2, 3–4, 5–6	99·2
TGTGT	$6B_2$	2–3, 4–5	148·3
TGTG$^-$T	$6B_2$	2–3, 4–5	135·7
TG$^-$TGT	$6B_2$	2–3, 4–5	129·8
TTGTG	$6B_2$	3–4, 5–6	121·7
TTG$^-$TG	$6B_2$	3–4, 5–6	120·6
TTTTT	$6M_6$		129·6
TGG$^-$GG$^-$	$6P_1$	2–3–4–5–6	73·5
2(TGG$^-$GG$^-$) 4(TGTGT)	$2P_1, 4B_2$		110·9

such as 6M$_6$ [Figure 3(b)], have 'tentacles' almost parallel to the CTP plane, and so are too open to enclose an IP aggregate. In other conformers, e.g. 6B$_2$ (TG$^-$TGT) [Figure 3(c)], the polyether chains stretch out of the CTP plane, marking the boundaries of a cavity, where the IP aggregates can enter, but the tentacles can also become twisted, closing the cavity completely.

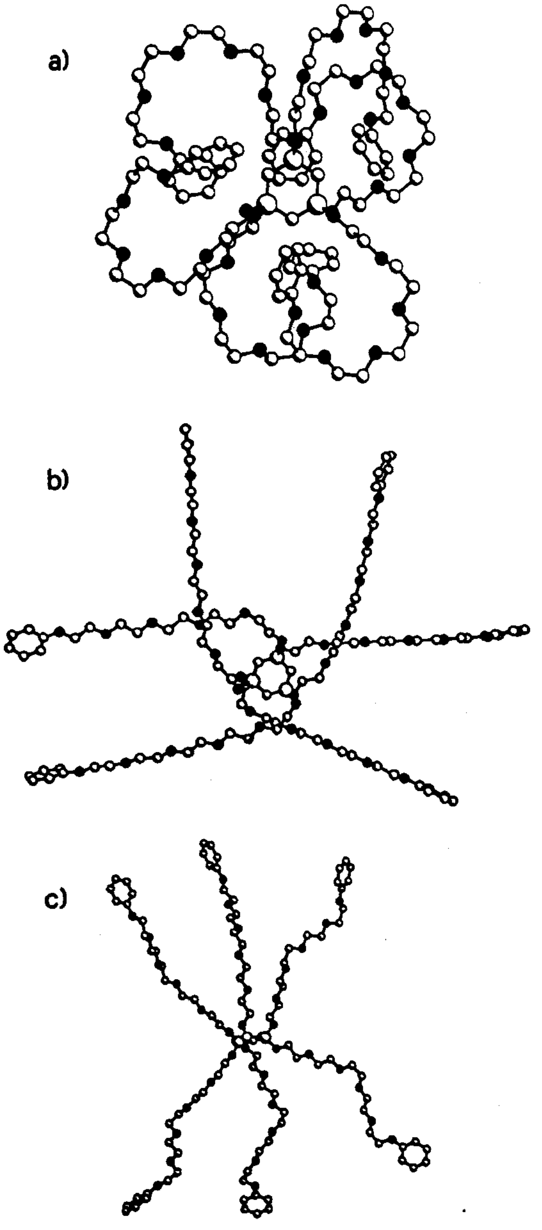

Figure 3. Plots of representative POD conformers: (a) 6P$_1$; (b) 6M$_6$; (c) 6B$_2$ (see text)

The conformers with polyether chains of the P$_1$ type are different from the others, as the twisted tentacles form pseudo-cavities oriented at an angle to the CTP plane, similar to the blades of a propeller, an example being the above-mentioned 6P$_1$ [Figure 3(a)]. Other conformers such as 2P$_1$ and 4B$_2$, with two pseudo-cavities occupy an intermediate position, having some tentacles stretched and others twisted.

Polypodands and aggregates of ion pairs

In order to understand the general features of the complexation of IP aggregates by polypodands, we performed calculations on (Li$^+$I$^-$)$_4$ complexes with POD (6B$_2$, TTG$^-$TG conformation) starting from two different conformations. In the first the IP aggregate is inserted between two chains attached to the same phosphorus, the (Li$^+$I$^-$)$_4$ symmetry axis and the bisector of OPO angle being coincident; this model describes the approach to the CTP ring in its plane. The second conformation corresponds to the arrangement of (Li$^+$I$^-$)$_4$ among three chains bound to different P atoms, the axis of symmetry of the IP aggregate and the C_3 axis of the CTP fragment being coincident; this model describes the perpendicular approach to the CTP ring. The second complex is more stable by 41·5 kcal mol^{-1}, because the chains on the same side of the CTP fragment give a cooperative contribution, while those on opposite sides act independently. As a consequence, it is possible to simulate the interaction of POD with ion pairs taking as a model its truncated analogue (T-POD), with three polyether chains on the side of the CTP fragment replaced with methoxy groups.

The conformers must provide the largest possible number of oxygen in order to bind IPs, and the molecules B$_2$ meet this requirement with the exception of TTG$^-$TG conformations. Free space is enclosed among the chains, so large aggregates (M$^+$I$^-$)$_n$ can enter this volume. The distances between O$_4$ atoms of different chains are in the range 12–19 Å, and those between O$_6$ atoms are in the range 16–23 Å. The sizes of the (M$^+$I$^-$)$_6$–(M$^+$I$^-$)$_8$ aggregates are 6–10 Å and the lengths of the M$^+\cdots$I$^-$ coordination bonds are 2–3 Å, so these conformers on the one hand have enough free space to capture IP aggregates and on the other allow effective interactions of IPs with the oxygen of three chains. The 6M$_1$ and 6B$_2$ (TTG$^-$TG) conformers do not meet these requirements, because the distances between the chains are too large, whereas for 6B$_3$ they are too short. The conformers with chains of P$_1$ types can interact only with one IP, and not with IP aggregates.

To analyse the formation of the complexes of polypodands with IP aggregates, the interaction of a T-POD molecule (TGTG$^-$T conformation) with (M$^+$I$^-$)$_4$ was modelled. The initial position of the (M$^+$I$^-$)$_4$ aggregate was set at the level of the O$_3$–O$_4$ atoms, a face of the IP cube and the plane of the CTP fragment being parallel and their axes of symmetry being coincident.

During the optimization, the $(M^+I^-)_4$ ($M^+ = Li^+, Na^+$) aggregates move to the region of the O_4–O_5 chelating BSs of two chains. The interaction with the ligand transforms the three-dimensional structure into a two-dimensional non-planar network [Figure 4(a)]; the cations of two IPs interact with the O_4–O_5 chelating BSs of two chains, whereas the other two IPs bridge the gap between them.

The interaction of the ligand with $(M^+I^-)_4$ ($M^+ = K^+, Rb^+$) is insufficient to induce large changes in the geometry of the aggregate; the cubic structure of $(K^+I^-)_4$ is only slightly deformed [Figure 4(b)] by the interaction with the O_4–O_5 chelating BSs of two chains, while the geometry of $(Rb^+I^-)_4$ remains unchanged.

Now let us consider the energetic aspects of the interaction of T-POD with $(M^+I^-)_4$ aggregates. Assuming that the solvation effects in chlorobenzene can be neglected, the complexation energy E_{comp} can be represented as

$$E_{\text{comp}} = \Delta E_{(M^+I^-)_4} + \Delta E_{\text{st}} + \Delta E_{L\cdots(M^+I^-)_4} \qquad (4)$$

where $\Delta E_{(M^+I^-)_4}$ and ΔE_{st} are the variations of the IP aggregate energy and of the ligand steric energy during the complexation process, and $\Delta E_{L\cdots(M^+I^-)_4}$ is the ligand–IP aggregate interaction energy. The results, reported in Table 5, show that the absolute value of the complexation energy decreases in the series $Li^+ > Na^+ > K^+ > Rb^+$, the differences in $|E_{\text{comp}}|$ being 27·5, 8·0 and 2·7 kcal mol^{-1}; these results might account for the dependence of n on M^+ in L–$(M^+I^-)_n$. It should be remembered that the experimental data obtained by titration[3] reveal not only the actual stoichiometry of the complexes in solution, but also their stability.

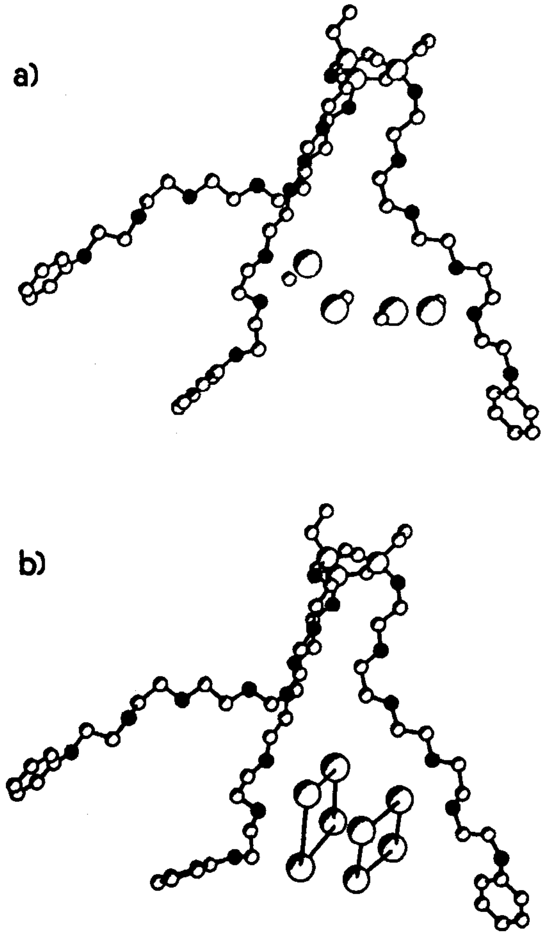

Figure 4. T-POD complexes with (a) $(Li^+I^-)_4$ and (b) $(K^+I^-)_4$

The effect of the transformation of the three-dimensional spatial structure of an IP aggregate into a two-dimensional non-planar network is also observed during the interaction of T-POD with $(Li^+I^-)_6$. The calculations were started locating the IP aggregate, parallelepiped in different positions. In a first model, $(Li^+I^-)_6$ shaped, was placed at the level of the O_4–O_5 atoms of the ligand chains, the largest face being parallel to the CTP plane. Under the influence of the ligand field, the parallelepiped 'melts' into a two-dimensional structure, which binds rigidly three O_4–O_5 chelating BSs of three chains [Figure 5(a)].

In a second model, $(Li^+I^-)_6$ was placed at the level of the O_2–O_3 atoms, with the smallest face of the parallelepiped parallel to a CTP-fragment plane. The three-dimensional structure of the IP aggregate is also destroyed, but a curved line of IPs connects the O_2–O_3 atoms of a chain with the O_4–O_5 atoms of two other chains [Figure 5(b)]. The first complex is more stable by 9·1 kcal mol^{-1}, as a result of an interaction energy lower by 14·6 kcal mol^{-1}, balanced by a steric energy lower by 23·8 kcal mol^{-1}. These results show that O_4–O_5 atoms play the most important role as far as binding of IP aggregates is concerned; they allow effective interactions with IP aggregates without large changes in the ligand steric energy.

The space among the chains in the $6B_2$ conformers

Table 5. Contributions to the complexation energy (kcal mol^{-1}) of T-POD with $(M^+I^-)_4$

Cation	$\Delta E_{(M^+I^-)_4}$	ΔE_{st}	$\Delta E_{L\cdots(M^+I^-)_4}$	E_{comp}
Li^+	4·0	19·5	−90·2	−66·7
Na^+	13·5	16·5	−69·2	−39·2
K^+	8·5	14·9	−54·6	−31·2
Rb^+	1·1	13·8	−43·4	−28·5

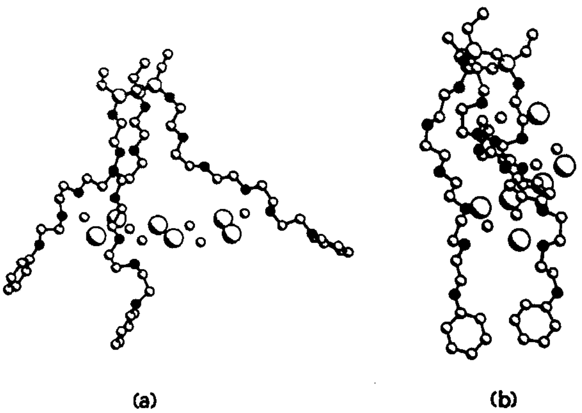

(a) (b)

Figure 5. T-POD complexes with $(Li^+I^-)_6$ (see text)

(see Figures 4 and 5) is large enough for capturing $(Li^+I^-)_n$ aggregates with $n > 6$. This fact and the strength of the lithium iodide–ligand interaction explain the fairly high values of n in $L-(Li^+I^-)_n$.[3]

Polypodands and single ion pairs

It is generally accepted that in low-polarity media the activation of the anion in complexes of macrocyclic ligands and of similar compounds is mainly due to the increased cation–anion separation in the ion pair.[2c,23] In the complexes of T-POD with IP aggregates, the cation–anion distance differs slightly from that typical of an isolated IP, so that the anion cannot be assumed to be activated, and other polypodand conformers, responsible for the activation, must be found. From the results for the glymes complexed with IPs it follows that only GLYME6 in the pseudo-cavity conformation (GG^-GG^-G) is able to interact so strongly with the cation of an IP to increase the distance between the counterions (Table 3). Similarly, one can assume that those POD conformers which include the maximum possible number of oxygens in a BS might show the same behaviour. The $6P_1$ conformer might be an example, because its BS is formed by five oxygens [Figure 3(a)].

Calculations were therefore performed on the complexes of a POD ($6P_1$) both with contact and ligand-separated IPs. In the former case, the starting distance $M^+\cdots I^-$ was set equal to the value of an isolated IP; in the latter, the anion was placed at a distance of 14 Å from the cation. The complexes with contact ion pairs $L(M^+I^-)$ are more stable than those with ligand-separated ion pairs $(M^+L)I^-$ (see Table 6), the relative stabilities being due to the different contributions to the interaction energy reported in Table 7. A cation separated from the anion by a large distance interacts with the ligand more effectively; however, the difference of the cation–anion interaction energy in $L(M^+I^-)$ and $(M^+L)I^-$ complexes is the main factor, so that the total effect is in favour of $L(M^+I^-)$.

In POD complexes with contact IPs, the interactions of the cations with their chains are weaker than with the pseudo-cavity of GLYME6. Li^+, Na^+ and K^+ cations interact efficiently with four oxygens of the chain and Rb^+ with five oxygens, whereas the other donor atoms are separated from M^+ by larger distances: 4·11 and 6·51 Å (Li^+), 4·28 and 6·42 Å (Na^+), 4·31 and 6·21 Å (K^+) and 5·07 Å (Rb^+). Simultaneously, some oxygens of other chains take part in the coordination, the corresponding $M^+\cdots O$ distances being 3·74, 6·56 Å (Li^+) 4·55 Å (Na^+), 6·29 Å (K^+) and 3·8, 5·6 Å (Rb^+), respectively. These additional interactions contribute to increase the absolute value of the interaction energy of K^+ and Rb^+ with POD with respect to GLYME6. The interactions of Li^+ and Na^+ with a chain in POD complexes are less effective than in GLYME6 complexes, causing the decrease of $|E_{M^+\cdots L}|$ on passing from glymes to polypodands (see Tables 3 and 7).

The interaction energy $E_{[LM^+]\cdots I^-}$ of the anion with the complexed cation $[LM^+]$, the sum of the $E_{M^+\cdots I^-}$ and $E_{L\cdots I^-}$ energies, should be a measure of the degree of anion activation by the ligand in the $L(M^+I^-)$ or $(LM^+)I^-$ complexes. The corresponding values for M^+I^- complexes with POD and GLYME6 are reported in Table 8, together with their equilibrium cation–anion distances. Only in the case of lithium iodide is the

Table 6. Total energies, E_{tot} (kcal mol^{-1}), and cation–anion distances, $R_{M^+\cdots I^-}$ (Å), of the complexes of POD (pseudo-cavity conformation) with alkali metal iodide ion pairs

	Contact IP		Separated IP	
Cation	E_{tot}	$R_{M^+\cdots I^-}$	E_{tot}	$R_{M^+\cdots I^-}$
Li^+	−148·6	6·32	−128·9	13·5
Na^+	−99·3	4·08	−69·6	14·4
K^+	−86·1	3·51	−53·3	14·2
Rb^+	−86·5	3·82	−47·0	14·2

Table 7. Cation–ligand, $E_{L\cdots M^+}$, anion–ligand, $E_{L\cdots I^-}$, and cation–anion, $E_{M^+\cdots I^-}$, interaction energies (kcal mol^{-1}) in the complexes of POD ($6P_1$) with alkali metal iodide ion pairs

	Contact IP			Separated IP		
Cation	$E_{L\cdots M^+}$	$E_{L\cdots I^-}$	$E_{M^+\cdots I^-}$	$E_{L\cdots M^+}$	$E_{L\cdots I^-}$	$E_{M^+\cdots I^-}$
Li^+	−189·4	−7·5	−52·5	−202·5	−5·8	−24·5
Na^+	−122·3	−13·6	−93·1	−130·4	−6·7	−23·0
K^+	−103·2	−11·0	−91·7	−106·0	−7·3	−23·3
Rb^+	−96·5	−8·3	−87·7	−98·0	−7·2	−24·2

Table 8. Anion–complex interaction energies, $E_{[\mathrm{LM}]^+\cdots\mathrm{I}^-}$ (kcal mol^{-1}), and cation–anion distances, $R_{\mathrm{M}^+\cdots\mathrm{I}^-}$ (Å), in the complexes of GLYME6 (pseudo-cavity conformation) and of POD (6P$_1$) with $\mathrm{M}^+\mathrm{I}^-$

	$E_{[\mathrm{LM}]^+\cdots\mathrm{I}^-}$		$R_{\mathrm{M}^+\cdots\mathrm{I}^-}$	
Cation	GLYME6	POD	GLYME6	POD
Li^+	−65·9	−60·0	5·73	6·32
Na^+	−72·0	−106·7	5·33	4·08
K^+	−85·3	−102·7	3·28	3·51
Rb^+	−82·1	−96·0	3·36	3·82

activation of the anion by a polypodand slightly higher than that by a glyme, whereas for Na, K and Rb iodides the opposite effect is observed. Such a difference should be ascribed to the different interactions among the components of the complex. Whereas in Li and Na complexes the corresponding changes in $E_{[\mathrm{LM}^+]\cdots\mathrm{I}^-}$ are determined by the differences in the cation–anion interaction energy $E_{\mathrm{M}^+\cdots\mathrm{I}^-}$, in K and Rb complexes the differences in the I^-–ligand interaction energies are of primary importance. This is the reason why $E_{[\mathrm{LM}^+]\cdots\mathrm{I}^-}$ correlates with $R_{\mathrm{M}^+\cdots\mathrm{I}^-}$ in $\mathrm{Li}^+\mathrm{I}^-$ and $\mathrm{Na}^+\mathrm{I}^-$ complexes, whereas such a correlation is absent in $\mathrm{K}^+\mathrm{I}^-$ and $\mathrm{Rb}^+\mathrm{I}^-$ complexes.

Mechanism and catalytic activity of neutral ligands under SL-PTC conditions

Overall, the present results show that, in the series of alkali metal iodides $\mathrm{M}^+\mathrm{I}^-$ ($\mathrm{M}^+ = \mathrm{Li}^+, \mathrm{Na}^+, \mathrm{K}^+, \mathrm{Rb}^+$), the degree of anion activation by polypodands (expressed as the reciprocal value of $|E_{[\mathrm{LM}^+]\cdots\mathrm{I}^-}|$) decreases in the order $\mathrm{Li}^+ \gg \mathrm{Rb}^+ > \mathrm{K}^+ > \mathrm{Na}^+$ (Table 8). This sequence is different from that previously found for the catalytic activity of **1a–c** in reaction (1) ($\mathrm{Li}^+ \gg \mathrm{Na}^+ > \mathrm{K}^+ > \mathrm{Rb}^+$).[3] This discrepancy can be easily explained considering that the catalytic activity depends also on the complexing ability of the ligand.[3] Indeed, the predicted complexation extents are in the same order as their complexation energies calculated for complexes T-POD with $(\mathrm{M}^+\mathrm{I}^-)_4$ ($\mathrm{Li}^+ \gg \mathrm{Na}^+ > \mathrm{K}^+ > \mathrm{Rb}^+$) (Table 5).

Our results allow reasonable hypotheses to be formulated about the possible mechanism of the catalytic activity of polypodands **1a–1c** and GLYME6 under SL-PTC conditions (reaction 1).

The catalyst, in a conformation L suitable for binding IP aggregates, initially interacts with $(\mathrm{M}^+\mathrm{I}^-)_n$, which is in dynamic equilibrium with the solid phase, giving the corresponding complex according to the equilibrium

$$(\mathrm{M}^+\mathrm{I}^-)_n + \mathrm{L} \rightleftharpoons [\mathrm{L}(\mathrm{M}^+\mathrm{I}^-)_n] \qquad (5)$$

This complex, through a conformational change (L′) of the polyether chains, rearranges in pseudo-cavities that can bind single ion pairs and hence activate the anion according to the equilibrium

$$[\mathrm{L}(\mathrm{M}^+\mathrm{I}^-)_n] \rightleftharpoons [\mathrm{L}'(\mathrm{M}^+\mathrm{I}^-)(\mathrm{M}^+\mathrm{I}^-)_{n-1}] \qquad (6)$$

(It is well known[26] that ion-pair aggregates are less reactive than single ion pairs in S_N2 reactions between anions and neutral molecules.)

Single ion pairs (experimental results confirm that the reactivity of $\mathrm{M}^+\mathrm{I}^-$ complexes of **1a–c** is comparable to that of analogous complexes of cyclic ligands (crown ethers), where the eventual presence of aggregates can be certainly excluded[27]) are the active species promoting reaction (1) in a relatively slow step of the overall process. According to our calculations, the conformer of the polypodand most suitable for binding IP aggregates (L) is 6B$_2$, whereas conformers containing chains of P$_1$ type (L′) are responsible for the anion activation.

The rearrangement L → L′ (equilibrium 6) is energetically favoured, as shown by the comparison of the interaction energies in the complex of POD (6P$_1$) with $\mathrm{Li}^+\mathrm{I}^-$ both in the case of four ion pairs (about 4 × 250 kcal mol^{-1}) (Table 7) and of the aggregate $(\mathrm{Li}^+\mathrm{I}^-)_4$ (about 600 kcal mol^{-1}) (Table 6). The steric energy of ligand with P$_1$ chains is also considerably lower than that of B$_2$ conformers (Table 4) (similar conclusions could apply also to complexes of polypodands **1a–c** with the other alkali metal iodides). These conclusions allow the prediction of the requirements to be met by neutral ligands in catalysing SL two-phase reactions: (i) polyether chains sufficiently long to effectively bind IP aggregates; and (ii) a high tendency to interact with the cation, thus activating the corresponding anion in the ion pair.

In this respect the polypodands **1b** and **1c** exhibit the best catalytic activity, as found experimentally.[3] The lower efficiency of GLYME6, in spite of its better anion activation (Table 8), is essentially due to the low tendency of this ligand to interact with IP aggregates. The decreased reactivity and the different stoichiometry $\mathrm{L}\text{–}(\mathrm{M}^+\mathrm{Y}^-)_n$ observed on passing from the alkali metal iodides to the corresponding bromides is probably due to both the smaller number of $(\mathrm{M}^+\mathrm{Br}^-)_n$ aggregates near the solid-phase surface and the higher binding energy in ion pairs. Therefore, the process of formation of $\mathrm{L}\text{–}(\mathrm{M}^+\mathrm{Br}^-)_n$ complexes and of anion activation becomes energetically less favoured in this case.

ACKNOWLEDGEMENT

We thank Professor S. S. Yufit (Institute of Organic Chemistry of the Russian Academy of Sciences) for fruitful discussions on the manuscript.

REFERENCES

1. F. Vögtle and E. Weber (Eds), *Host–Guest Complex Chemistry – Macrocycles. Synthesis, Structure, Applications*. Springer, Berlin (1985).
2. (a) C. M. Starks and C. L. Liotta, *Phase-Transfer Catalysis: Principles and Applications*, Academic Press, New York (1978); (b) F. Montanari, D. Landini and F. Rolla, *Top. Curr. Chem.* **101**, 147 (1982); (c) E. V. Dehmlow and S. S. Dehmlow, *Phase-Transfer Catalysis*, 2nd ed. Verlag-Chemie, Weinheim (1983); (d) S. S. Yufit, *Phase Transfer*. Nauka, Moscow (1984); (e) F. M. Menger, *Top. Curr. Chem.* **136**, 1 (1986); (f) M. Makosza and M. Fedorynski, *Adv. Catal.* **35**, 375 (1988); (g) Y. S. Goldberg, *Selected Chapters of Phase-Transfer Catalysis*. Znanie, Riga (1989); (h) T. E. Kron and E. N. Tsvetkov, *Russ. Chem. Rev.* **59**, 283 (1990).
3. (a) D. Landini, A. Maia, L. Corda, A. Maccioni and G. Podda, *Tetrahedron Lett.* **30**, 5781 (1989); (b) *Tetrahedron* **47**, 7477 (1991).
4. S. S. Yufit and I. A. Esikova, *J. Phys. Org. Chem.* **4**, 149, 336, 341 (1991) and references cited therein.
5. G. A. Krestov (Ed.), *Ion Solvation*, Nauka, Moscow (1987).
6. Ya. Yu. Akhadov, *Dielectric Properties of Binary Solutions*. Pergamon Press, Oxford (1981).
7. A. A. Varnek, A. S. Glebov, O. M. Petrukhin and R. P. Ozerov, *Koord. Khim.* **15**, 600, 740 (1989).
8. N. L. Allinger, *J. Am. Chem. Soc.* **99**, 8127 (1977).
9. H. R. Allcock, D. C. Ngo, M. Parvez, R. R. Whittle and W. J. Birdsall, *J. Am. Chem. Soc.* **113**, 2628 (1991).
10. V. A. Naumov and L. V. Vilkov, *Molecular Structures of Organophosphorus Compounds*. Nauka, Moscow (1986).
11. J. Caillet and P. Claverie, *Acta Crystallogr., Sect. A* **31**, 448 (1975).
12. N. Gresh, P. Claverie and A. Pullman, *Int. J. Quantum Chem. Symp.* **13**, 243 (1979).
13. S. R. Cox and D. E. Williams, *J. Comput. Chem.* **2**, 304 (1981).
14. M. L. Connolly, *J. Appl. Crystallogr.* **16**, 548 (1983).
15. *MOPAC-5 QCPE Program No. 589*. Department of Chemistry, Indiana University, Bloomington, IN (1990).
16. B. H. Besler, K. M. Merz and P. A. Kollman, *J. Comput. Chem.* **11**, 432 (1990).
17. R. J. Woods, M. Khalil, W. Pell, S. H. Moffat and V. H. Smith, Jr, *J. Comput. Chem.* **11**, 298 (1990).
18. P. D. J. Grootenhuis and P. A. Kollman, *J. Am. Chem. Soc.* **111**, 2152 (1989).
19. A. A. Varnek, G. Morosi and A. Gamba, *J. Phys. Org. Chem.* **5**, 109–118 (1992).
20. R. J. M. Le Fevre, *Adv. Phys. Org. Chem.* **3**, 1 (1965).
21. A. Yu. Tsivadze, A. A. Varnek and V. E. Khutorsky, *Coordination Compounds of Metals with Crown Ligands*. Nauka, Moscow (1991).
22. K. P. Huber and G. Herzberg, *Molecular Spectra and Molecular Structure. Constants of Diatomic Molecules*, p. 716, Van Nostrand, New York (1979).
23. S. I. Drakin and M. Kh. Karapetyants, *Structure of Matter*. Vischaya Schkola, Moscow (1973).
24. N. R. Sreltsova, A. A. Varnek, A. S. Glebov and V. K. Belsky, in *Crystallochemistry Problems*, edited by M. Porii-Koshits, p. 47. Nauka, Moscow (1989).
25. K. Matsuzaki and H. Ito, *J. Polym. Sci. Polym. Phys. Ed.* **27**, 2507 (1974).
26. (a) J. E. Gordon, *The Organic Chemistry of Electrolyte Solution*, Chapt. 3, Wiley, New York (1975); (b) N. S. Isaacs, *Physical Organic Chemistry*, Chapt. 1. Longman, Harlow (1987); (c) M. Crescenzi, C. Galli and M. Mandolini, *J. Phys. Org. Chem.* **3**, 428 (1990).
27. D. Landini, A. Maia, G. Podda, D. Secci and Y. M. Yan, *J. Chem. Soc. Perkin Trans. 2*, 1721 (1992).